Discovery of novel N-(5-(tert-butyl)isoxazol-3-yl)-N'-phenylurea analogs as potent FLT3 inhibitors and evaluation of their activity against acute myeloid leukemia in vitro and in vivo

Ying Xu [a,†], Ning-Yu Wang [a,†], Xue-Jiao Song [a], Qian Lei [a], Ting-Hong Ye [a], Xin-Yu You [a,b], Wei-Qiong Zuo [a], Yong Xia [a], Li-Dan Zhang [a,b], Luo-Ting Yu [a,*]

[a] State Key Laboratory of Biotherapy and Cancer Center, West China Hospital, Sichuan University, and Collaborative Innovation Center for Biotherapy, Chengdu 610041, China
[b] College of Chemical Engineering, Sichuan University, Chengdu, Sichuan 610065, China

ARTICLE INFO

ABSTRACT

FLT3 inhibitors have been explored as a viable therapy for acute myeloid leukemia (AML). However, the clinical outcomes of these FLT3 inhibitors were underwhelming except AC220. Therefore, the development of novel FLT3 inhibitors with high potency against both FLT3-WT and FLT3-ITD mutants are strongly demanded at the present time. In this study, we designed and synthesized a series of novel N-(5-(tert-butyl)isoxazol-3-yl)-N'-phenylurea derivatives as FLT3 inhibitors. SAR studies focused on the fused rings led to the discovery of a series of compounds with high potency against FLT3-ITD-bearing MV4-11 cells and significantly inhibitory activity toward FLT3. Among these compounds, N-(5-(tert-butyl)isoxazol-3-yl)-N'-(4-(7-methoxyimidazo[1,2-a]pyridin-2-yl)phenyl)urea (**16i**), displayed acceptable aqueous solubility, desirable pharmacokinetic profile and high cytotoxicity selectivity against MV4-11 cells. This compound can inhibit phosphorylation of FLT3 and induce apoptosis in a concentration-dependent manner. Further in vivo antitumor studies showed that **16i** led to complete tumor regression in the MV4-11 xenograft model at a dose of 60 mg/kg/d while without observable body weight loss. This study had provided us a new chemotype of FLT3 inhibitors as novel therapic candidates for AML.

© 2015 Published by Elsevier Ltd.

1. Introduction

FMS-like tyrosine kinase 3 (FLT3), a member of the class III receptor tyrosine kinase family, is mainly expressed on hematopoietic system, nervous system, gonads and placenta.[1,2] In the hematopoietic system, FLT3 is a key mediator of early haematopoiesis and plays several important roles in the proliferation, differentiation and apoptosis of hematopoietic cells.[3,4] Over-expression of FLT3, or its constitutive activation, appears to play a major role in the development and progress of leukemia, especially in acute myeloid leukemia (AML).[5] Actually, approximately 90% of AML patients have been found over-expression of FLT3. While some of these patient-derived AML cells exhibit over-expression of FLT3-WT, others are found to harbor activating mutations of FLT3.[6] There are two major classes of activating mutations of FLT3, internal tandem duplications (ITDs) in the juxtamembrane domain of the receptor and 'activation loop' mutations in the activation loop

of the tyrosine kinase domain, which are found in approximately 23% and 7% of patients with AML, respectively.[7,8]

FLT3-ITD mutations trigger constitutive activation of FLT3, which activated downstream signaling cascades and resulted in survival and proliferation of leukemic cells.[9] Besides, the over activation of FLT3 by FLT3-ITD mutants is relevant to a poor prognosis and the complete remission rate of patients with FLT3-ITD mutations is much lower than that of patients with FLT3-WT when treated with conventional chemotherapy like cytarabine and anthracycline.[10,11] Therefore, FLT3 presents us an attractive target for the treatment of AML, especial patients with FLT3-ITD mutations. And FLT3 inhibitors have emerged in a rash in recent years for the treatment of AML patients.[12]

The first panel of FLT3 inhibitors nearly all belong to multi-kinase inhibitors. Several of them, such as sunitinib (SU-11248),[13] sorafenib (BAY-43-900),[14] tandutinib (MLN518),[15] lestaurtinib (CEP-701),[16] midostaurin (PKC412)[17] and KW-2449[18] (Fig. 1) have been advanced to clinical trials as potential drug candidates for AML patients.[19] However, the clinical outcomes of these FLT3 inhibitors is far from being satisfactory, probably due to their inability of completely and sustained inhibition of FLT3 in vivo.[20] Thus, the
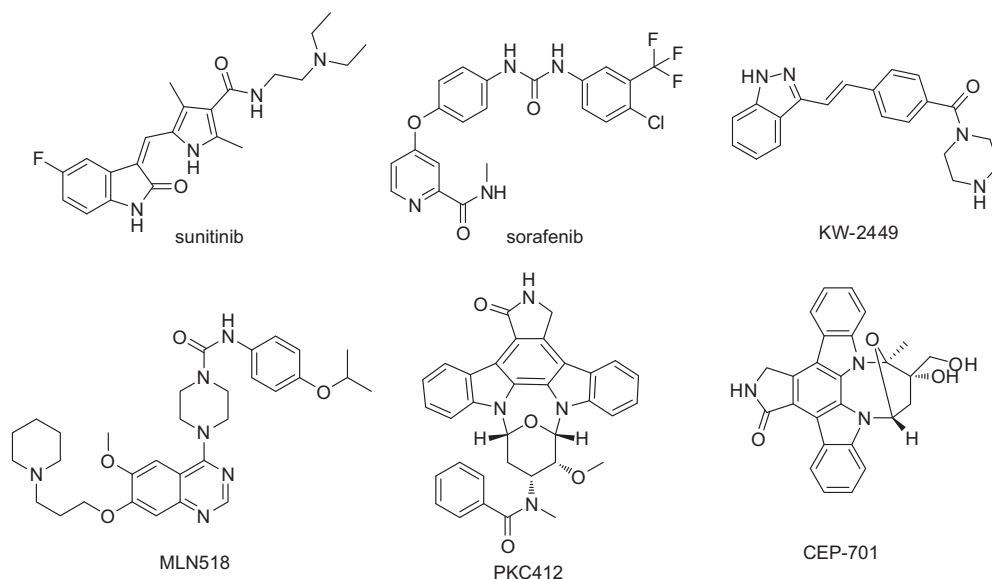
Figure 1. Structure of known FLT3 inhibitors.

development of novel FLT3 inhibitors with high potency and selectivity against both FLT3-WT and FLT3-ITD mutants are urgent needed at the present time.

To date, AC220 (Fig. 2), a second generation selective FLT3 inhibitor, is one of the most potential clinical candidate for AML. Moreover, the excellent kinase selectivity implied that it represented an attractive new class of drug candidates for the treatment of FLT3-ITD patients with relapsed and refractory AML.[21] Our research group aimed at developing novel second generation FLT3 inhibitors. In this study, a series of novel N-(5-(tert-butyl)isoxazol-3-yl)-N′-phenylurea derivatives (Fig. 2) were designed via the principle of isostere based on AC220. Herein, we describe the chemical synthesis, structure–activity relationship (SAR) investigation and biologic evaluation of this new kind of compounds.

2. Chemistry

The synthesis of our analogs was outlined in Schemes 1 and 2. As shown in Scheme 1, the intermediates **2**, **4**, **6**, **8** and **11** were prepared through five different routes. Briefly, condensation of **1** with 4-nitrobenzaldehyde in the presence of [bis(trifluoroacetoxy)iodo]benzene (PIFA) provided **2**.[22] Benzo[b]thiophene intermediate **4** was formed using a Suzuki coupling of **3** and 1-bromo-4-nitrobenzene.[23] Then benzofuran derivative **6** was achieved by reacting **5** with 4-nitrobenzyl bromide in refluxing DMF, while condensation of different heterocyclic **7** with 2-bromo-4′-nitroacetophenone gave various N-contained fused rings **8**.[24] Finally, coupling of **9** with bis(pinacolato)diboron followed by H_2O_2 treatment yielded **10**, which was alkylated with iodoalkane or acylated with acyl chloride under basic condition provided **11**.

Scheme 2 depicted the general reaction route of the target products. The key building blocks **12** were first reduced with iron powder and then coupled with 5-tert-butyl-isoxazole-3-isocyanate **14**, which was achieved by reacting 3-amino-5-tert-butyl-isoxazole with triphosgene, to yield the ureas **15** and **16**.[25]

2.1. Structure–activity relationship (SAR) analysis

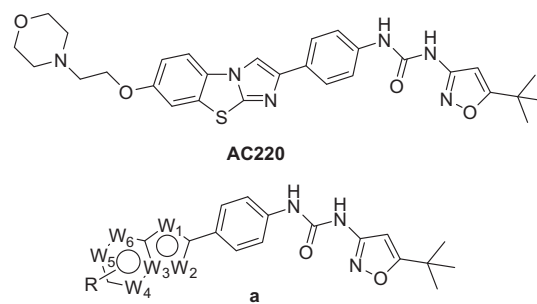In our initial SAR study, various fused rings were introduced to the para-position of the phenyl to find a suitable scaffold in this position. As show in Table 1, a series of nitrogen-contained bicyclic derivatives was first synthesized and evaluated for its FLT3 inhibitory activity as well as the in vitro antiproliferative activity. **15a**, which contains an imidazo[1,2-a]pyridine substituent at phenyl, was found to potently inhibit MV4-11 (IC_{50} = 3.09 nM) and FLT3 (65.7% inhibition at 100 nM). While **15b**–**15d**, which contain imidazo[1,2-a]pyrimidine substituent, imidazo[1,2-a]pyrazine substituent and imidazo[1,2-b]pyridazine substituent, respectively, were about 15–50 fold less potent than **15a** in with respect to antiproliferative activity against MV4-11. This probably due to the lower electron cloud density of these fused rings compared with imidazo[1,2-a]pyridine ring. Having demonstrated the importance of the electron-rich group, we then focused on the oxygen-contained and sulfur-contained bicyclic derivatives. Likewise, the cytotoxicity against MV4-11 of **15e** (benzo[b]thiophene, IC_{50} > 900 nM), **15f** (benzofuran, IC_{50} > 195.14 nM), **15g** (benzo[d]oxazole, IC_{50} = 82.57 nM) and **15h** (benzo[d]thiazole, IC_{50} = 172.31 nM) were dramatic decreased compared with **15a**, indicating that the N4 position of the imidazo[1,2-a]pyridine ring was important for the activity. In addition, compared with compounds **15f**–**15h**, the potency of **15e** was absolutely lost, which might be due to its shortage of a hydrogen bond acceptor at the bicyclic fragment.

Since the cellular activity of imidazo[1,2-a]pyridine substituent **15a** was the best among the first batch of compounds, our next SAR study focused on four positions of the imidazo[1,2-a]pyridine ring

Figure 2. Structure of AC220 and **a**.
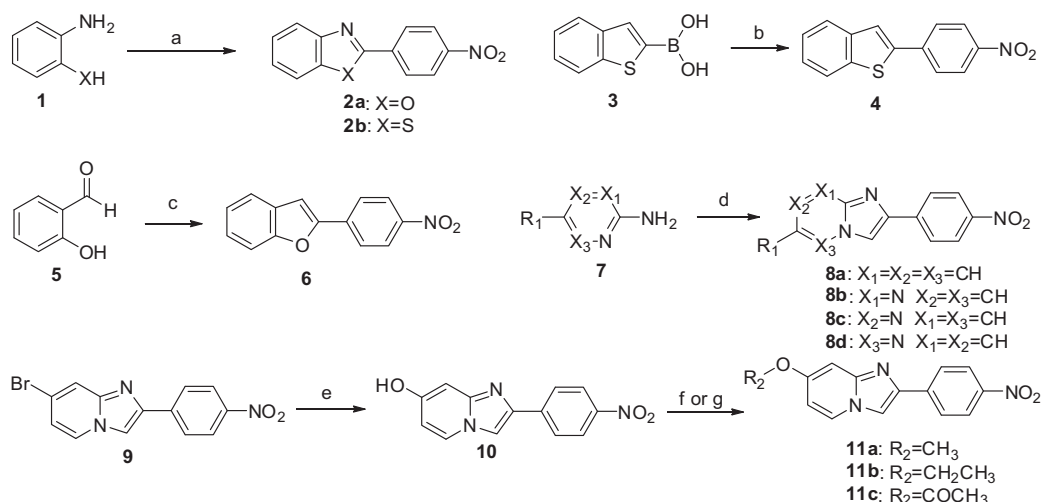
Scheme 1. Reagents and conditions: (a) (i) 4-nitrobenzaldehyde, grinding, rt; (ii) PIFA, grind, rt; (b) 1-bromo-4-nitrobenzene, $Na_3PO_4 \cdot 12H_2O$, 10% Pd/C (1.0 mol %), i-PrOH, 80 °C; (c) 4-nitrobenzyl bromide, K_2CO_3, DMF, reflux; (d) 2-bromo-4′-nitroacetophenone, EtOH, reflux; (e) (i) bis(pinacolato)diboron, CH_3COOK, $PdCl_2(dppf)$, 1,4-dioxane, 100 °C; (ii) H_2O_2, H_2O; (f) CH_3I or CH_3CH_2I, K_2CO_3, DMF; (g) DMAP, CH_2Cl_2, CH_3COCl.
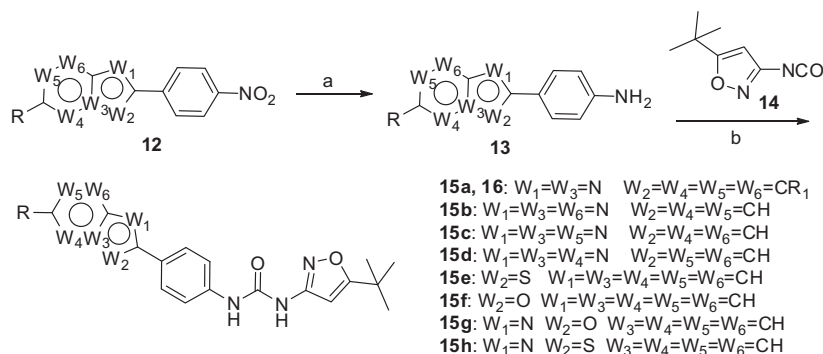
Scheme 2. Reagents and conditions: (a) Fe, NH_4Cl, H_2O/EtOH, reflux; (b) $CHCl_3$, 60 °C.

(Fig. 3). Various derivatives of **15a** together with their bioactivities were presented in Table 2.

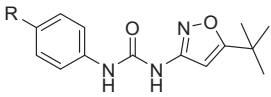The H atom at C8 position of imidazo[1,2-a]pyridine ring was replaced by fluorine, chlorine, methyl and trifluoromethyl group, yielding compounds **16a–16d**, respectively. As show in Table 2, compounds **16a** (IC_{50} = 12.21 nM), **16b** (IC_{50} = 352.76 nM), **16c** (IC_{50} = 248.42 nM) and **16d** (IC_{50} > 900 nM) exhibited much lower anti-proliferative and anti-FLT3 activities than their unsubstituted counterpart **15a** and the antiproliferative activity decreased as the size of the substituent increasing. Moreover, it's worth noting that a trifluoromethyl introduced to this position led to an inactive compound (**16d** IC_{50} > 900 nM), indicated that a bulky substituent at this position was detrimental to the potency against MV4-11 and FLT3.

Next, a series of substituents were introduced in C7 position to study their influence on the potency. The results show that the introduction of chlorine (**16e**, IC_{50} = 5.91 nM), bromine (**16f**, IC_{50} = 9.59 nM), methyl (**16g**, C_{50} = 0.79 nM) or ethynyl (**16h**, IC_{50} = 3.46 nM) at this position was well tolerated. Moreover, the methyl and ethynyl analogs **16g** and **16h** displayed a better inhibitory activity in the cellular assay than their chlorine and bromine counterparts **16e** and **16f**, suggesting that electron-donating substituent at this position was superior to electron-withdrawing substituent. Methoxy substituent analog **16i** maintained excellent anti-MV4-11 activity with an IC_{50} value of 2.84 nM while incorporation of ethoxy and acetoxy group at this position resulted in 4–10 fold decrease of potency compared with **16i** (**16j**, IC_{50} = 11.59 nM and **16k**, IC_{50} = 29.39 nM).

We then explored the influence of different substituents at C6 position. When this position was substituted with halogen groups, the resulting compounds **16l** (fluorine, IC_{50} = 20.94 nM), **16m** (chlorine, IC_{50} = 24.75 nM), **16n** (bromine, IC_{50} = 44.48 nM) and **16o** (iodine, IC_{50} = 98.55 nM) showed a 7–30 fold loss of potency against MV4-11 compared with the unsubstituted counterpart **15a**. And the potency against MV4-11 was decreased along with the increasing size of the substituent. Furthermore, the antiproliferative activity was reserved as the introduction of a methyl (**16p**, IC_{50} = 4.08 nM) or an ethynyl (**16q**, IC_{50} = 8.62 nM) to this position, while 5 fold loss of potency was observed when a cyclopropane was introduced (**16r**, IC_{50} = 15.83 nM), which indicated that a relative large cycloalkyl group at this position was disadvantage to the potency against MV4-11 and FLT3. Interestingly, the cell growth inhibitory activities against MV4-11 of the electron-donating derivatives **16p**, **16q** and **16r** were higher than that of the electron-withdrawing derivatives **16l–16o**, which was consistent with the SAR of C7 position. These results further supported the conclusion that an electron-rich bicyclic motif was important for the antiproliferative activity as well as FLT3 inhibitory potency.

Lastly, in order to explore the substitution effect of C5 position of imidazo[1,2-a]pyridine ring, we synthesized compounds **16s–16t** that contained different substituents at this position. The bioactivity of **16s–16t** at the cellular level was clearly decreased relative to their counterpart **15a** (Table 2), which suggested that substitution at this position was not beneficial for increasing the bioactivity against MV4-11.

Table 1
SAR of derivatives with varied fused rings

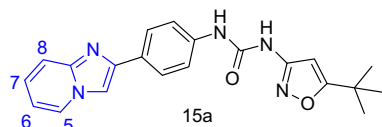| Compd	R	MV4-11 (IC$_{50}$, nM)	FLT3 (inhibition at 100 nM, %)
AC220	–	0.68	69.3
15a		3.09	65.7
15b		170.68	19.9
15c		44.83	35.5
15d		59.05	30.9
15e		>900	3.8
15f		195.14	11.5
15g		82.57	21.8
15h		172.31	14.7

Figure 3. The structure of compound **15a** and the four regions our SAR study focused on.

Collectively, the structural optimization and SAR studies led to the discovery of a series of compounds which exhibited superior potency against human AML MV4-11 cells and delightful inhibition of FLT3. Then we studied the solubility of the most potent compounds **15a**, **16g**, **16h** and **16i** in several organic solvent and water. As show in Table 3, all of these compounds were well soluble in organic solvent, while compound **16i** was significantly more soluble than compounds **15a**, **16g** and **16h** in water. Thus, **16i** was selected to carry out further PK profile, in-depth in vitro and in vivo anti-AML studies.

2.2. Pharmacokinetic assays

The preliminary pharmacokinetic characteristic of **16i** following oral administration to rats was analyzed. As shown in Table 4, at an oral dose of 30 mg/kg, **16i** demonstrated desirable maximum plasma level (C_{max} 3.29 mg/L), favorable drug exposure (AUC$_{0-24h}$ 14.32 mg/L·h) and moderate apparent plasma half-life ($T_{1/2}$ 4.86 h), indicating that **16i** was orally available for tumor xenograft studies in vivo.

2.3. In vitro cell growth inhibitory activity of 16i

To further study the growth inhibitory potencies of compound **16i**, a panel of human cancer cell lines originated from different tissue, including leukemia and solid tumor, were treated with **16i** and the results are presented in Table 5. **16i** potently inhibited the growth of FLT3-ITD-bearing MV4-11 cells, with an IC$_{50}$ value of 0.003 μM. While it just exhibited very weak antiproliferative activity against human acute monocytic leukemia THP-1 cells and human lung cancer A549 cells (IC$_{50}$ of 3.37 μM and 5.61 μM, respectively). For other cancer cell lines, including K562, U937, Jurkat, MCF-7, PANC-1, U251, HepG2, A875 and HCT116, **16i** only exhibited a negligible growth inhibition effect at the concentration of 20 μM (Table 5). Furthermore, the viability of MV4-11 cells was attenuated along with increasing concentration of **16i** and duration of exposure (Fig. 4a). These data suggested that **16i** was highly selective for the human AML cell line MV4-11 and inhibited MV4-11 cells proliferation in a dose- and time-dependent manner.

2.4. Phosphorylation of FLT3 and apoptosis assays in MV4-11 cells

To examine whether **16i** inhibited phosphorylation of FLT3 in intact cells, MV4-11 cells were treatment with increasing concentrations of **16i** for 2 h, and the level of FLT3 as well as phosphorylated FLT3 was determined by Western blot (Fig. 4b). It was found that **16i** inhibited FLT3 phosphorylation in a dose-dependent manner without observable influence on FLT3 expression. Then flow cytometry assay was further performed to examine the apoptosis inducing effect upon treatment with **16i** for 48 h. As shown in Figure 4c, **16i** increased the percentage of apoptotic cells (positive Annexin V-FITC and negative PI staining) in a dose-dependent manner, and at a concentration of 100 nM, the early stage apoptosis rate and late stage apoptosis rate were 6.9% and 23%, respectively.

2.5. In vivo efficacy and immunohistochemical analysis

Finally, in vivo anti-AML activity of **16i** was evaluated using the FLT3-ITD-bearing MV4-11 xenograft model. Oral administration of **16i** at dose of 10, 30 and 60 mg/kg once a daily were initiated when the tumor grew to a volume of 100–200 mm³, and the tumor volumes were measured every 3 days. As shown in Figure 5a, at the dose of 60 mg/kg/d, **16i** was able to yield complete regression of established tumors during the dosing period. In addition, **16i** substantially suppressed tumor growth in a dose-dependent manner with inhibition rates of 51% and 87% at 10 mg/kg/d and 30 mg/kg/d, respectively. Moreover, no significant weight loss (Fig. 5b) or any other obvious signs of toxicity were observed for all of the **16i**-treated mice during the whole study.

The effects of **16i** on cancer cell proliferation and apoptosis were also evaluated using immunohistochemical assays. Mice bearing MV4-11 xenograft tumors were treated orally once daily with 60 mg/kg/d of **16i**, and tumor tissue were collected and analyzed 7 days later. Tumor tissues from the vehicle group were stained strongly with Ki67, indicating a large number of highly proliferative cells (Fig. 5c). Conversely, tumor tissues from the **16i**-treated groups showed significantly fewer Ki67-positive cells. Furthermore, the TUNEL assay of the **16i**-treated groups showed an obvious increase of apoptotic cells compared with the vehicle group (Fig. 5c).

3. Conclusion

In this paper, we designed and synthesized a series of novel N-(5-(tert-butyl)isoxazol-3-yl)-N′-phenylurea derivatives based on the FLT3 inhibitor AC220 through bioisostere principle. Structure–activity relationship studies demonstrated that an electron-rich fused ring at the phenyl was beneficial for the

Table 2
SAR of carried substitutions at the imidazo[1,2-a]pyridine
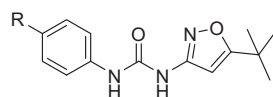
Compd	R	MV4-11 (IC$_{50}$, nM)	FLT3 (inhibition of 100 nM, %)
15a		3.09	65.7
16a		12.21	38.9
16b		352.76	12.5
16c		248.42	13.6
16d		>900	2.5
16e		5.91	44.2
16f		9.59	39.5
16g		0.79	69.0
16h		3.46	57.8
16i		2.84	57.4
16j		11.59	44.2
16k		29.39	27.4
16l		20.94	31.8
16m		24.75	35.7
16n		44.48	28.4
16o		98.55	29.3
16p		4.08	48.8
16q		8.62	39.9
16r		15.83	30.5

Table 2 (continued)
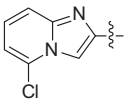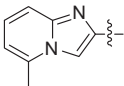
Compd	R	MV4-11 (IC$_{50}$, nM)	FLT3 (inhibition of 100 nM, %)
16s		56.08	28.5
16t		20.24	41.5

Table 3
The solubility of compounds **15a**, **16g**, **16h** and **16i** in different solvent

Compd	μg/mL				
	MeOH	EtOH	H$_2$O	PBS	SPSS
15a	5276	4072	ND[a]	ND[a]	ND[a]
16g	6827	3340	ND[a]	ND[a]	ND[a]
16h	5842	4105	26.7	10.2	ND[a]
16i	7460	3149	303.6	36.6	1.47

[a] ND: not detected.

Table 4
Pharmacokinetic parameters of 16i in rats[a]

Compd	Parameter				
	AUC$_{0-24h}$ (mg/ L·h)	C$_{max}$ (mg/ L)	t$_{1/2}$ (h)	Vd$_{ss}$ (L/ kg)	CL (L/h/ kg)
16i	14.32	3.29	4.86	14.12	2.01

[a] Sprague–Dawley rats were dosed at 30 mg/kg po (n = 3).

Table 5
Antiproliferative activities of **16i** against various cell lines

Cell lines	Tumor type	IC$_{50}$ (μM)
MV4-11	Human acute myeloid leukemia	0.003
K562	Human chronic myelogenous leukemia	>20
U937	Human leukemic monocyte lymphoma	>20
THP-1	Human acute monocytic leukemia	3.37
Jurkat	Human T lymphoma	>20
A549	Human lung cancer	5.61
MCF-7	Human breast cancer	>20
PANC-1	Human pancreatic carcinoma	>20
U251	Human glioma	>20
HepG2	Human hepatic cancer	>20
A875	Human melanoma	>20
HCT116	Human colorectal carcinoma	>20

antiproliferative activity and the introduction of substituents in C6 and C7 position were more tolerated than in C5 and C8 position. Four compounds (**15a**, **16g**, **16h** and **16i**) showed superior potency against FLT3-ITD-bearing MV4-11 cells (IC$_{50}$ = 3.09, 0.79, 3.46 and 2.84 nM, respectively) and delightful inhibition of FLT3. Among these compounds, **16i** displayed well aqueous solubility, desirable pharmacokinetic profile and high selectivity against MV4-11 cells. Further in vivo anti-AML activity assays showed that **16i** led to complete tumor regression in the MV4-11 xenograft model at a dose of 60 mg/kg/d. In addition, western blot, apoptosis and immunohistochemical analysis demonstrated that **16i** could downregulate the phosphorylation of FLT3, induced apoptosis and block the proliferation of MV4-11 cell in vitro and in tumor tissue. Our preliminary optimization of this new chemotype of FLT3 inhibitors had provided us novel drug candidates for AML, and further lead optimization as well as biologic studies are underway.

4. Experimental section

4.1. Chemistry methods

^{1}H and ^{13}C NMR spectra were generated in DMSO-d_6 on a Bruker AVANCE^{III} 400. Chemical shifts (δ) were reported in ppm relative to Me$_4$Si (internal standard), and coupling constants (J) were reported in Hz. Low-resolution mass spectra (ESI) were performed on a Bruker Amazon SL ESI mass spectrometer. HPLC conditions were as follows: column, Agilent Eclipse Plus C18 3.5 μM, 4.6 mm × 150 mm; solvent system, ACN/H$_2$O; flow rate 1.0 ml/min; UV detection, 270 nM; injection volume, 5 μL; temperature, 30 °C. All tested compounds were purified until the purity was ⩾95%, detected by HPLC, NMR and ESI-MS.

4.1.1. General procedure for the preparation of intermediates
4.1.1.1. General procedure for the preparation of 2.
A mixture of **1** (1.0 equiv) and 4-nitrobenzaldehyde (1.0 equiv) was blended thoroughly in pestle with mortar for 2 min. Then we added [bis(trifluoroacetoxy)iodo]benzene (PIFA, 1.2 equiv) and ground the reaction mixture for 3 min. After completion of reaction, reaction mixture was triturated with hexane to remove iodobenzene. Then we added cold saturated NaHCO$_3$ to quench the reaction and filtered the product. The solid thus obtained was recrystallized with methanol to afford **2**.

4.1.1.2. General procedure for the preparation of 4.
To a mixture of benzo[b]thiophen-2-ylboronic acid **3** (1.5 equiv) and 1-bromo-4-nitrobenzene (1.0 equiv) in isopropanol/H$_2$O (v/v: 10:1), Na$_3$PO$_4$·12H$_2$O (3.5 equiv) and 10% Pd/C (0.05 equiv) were added, and the mixture was stirred under nitrogen at 80 °C for 4 h. After completion of reaction, the mixture was diluted with H$_2$O and acetic ether, and filtered through a filter. The filtrate was separated into two layers and the aqueous layer was extracted with acetic ether. Then the combined organic layers were dried over MgSO$_4$ and concentrated under vacuum. The residue was purified by silica gel chromatography to give **4**.

4.1.1.3. General procedure for the preparation of 6.
A solution of 2-hydroxybenzaldehyde (1.0 equiv), 4-nitrobenzyl bromide (1.0 equiv), and K$_2$CO$_3$ (3.0 equiv) in DMF was stirred under reflux overnight. After completion of reaction, the solvent was removed and the residue was recrystallized with ethyl acetate to give **6**.

4.1.1.4. General procedure for the preparation of 8.
A mixture of pyridine amine **7** (1.0 equiv) and 2-bromo-4′-nitroacetophenone (1.1 equiv) in ethanol was heated to reflux overnight. The solution was then allowed to stand at room temperature for 2 h. The precipitate was collected by filtration, washed with methanol and dried under vacuum to give **8**.

4.1.1.5. General procedure for the preparation of 11a and 11b.
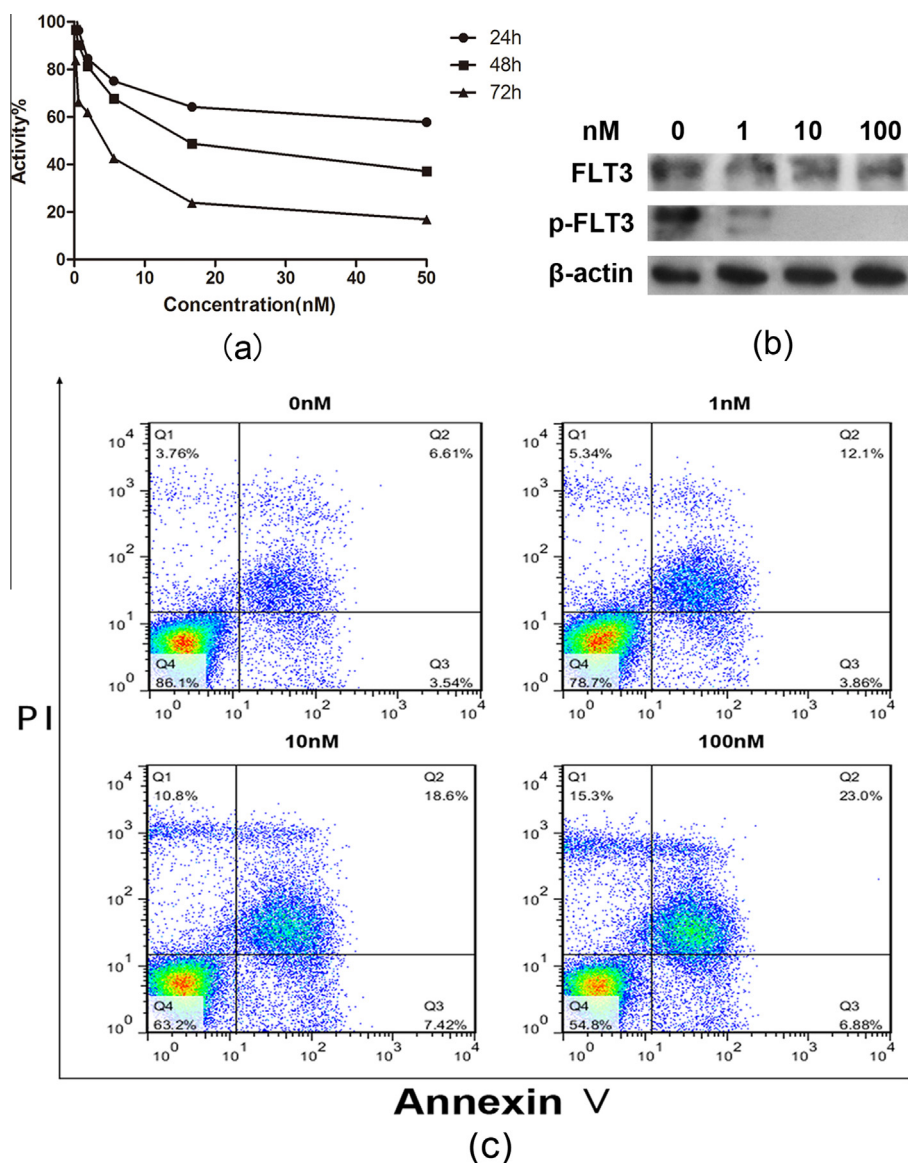7-Bromo-2-(p-tolyl)imidazo[1,2-a]pyridine (**9**, 1.0 equiv),

Figure 4. (a) MV4-11 cells were treated with different concentrations of **16i** for 24–72 h and cell viability was determined by MTT assay. (b) Western blot analysis was used to examine the expression and phosphorylation of FLT3 in MV4-11 cells treated with different doses of **16i** for 2 h. (c) Flow cytometric analysis of cells stained with Annexin V-FITC/PI after treatment with various concentrations (0 nM, 1 nM, 10 nM, 100 nM) of **16i** for 48 h.

potassium acetate (3.0 equiv), bis(pinacolato)diboron (2.25 equiv) and PdCl$_2$(dppf) (0.1 equiv) in 1,4-dioxane were heated to 100 °C for 2 h. The mixture was cooled to room temperature before acetic acid (2.0 equiv) and water were added. The mixture was stirred for 1 h and 30% hydrogen peroxide (2.0 equiv) was added. After 3 h, the precipitate was collected by filtration, washed with EtOH and dried under vacuum to give **10**.

Then **10** (1.0 equiv), potassium carbonate (2.0 equiv) and methyl iodide or ethyl iodide (1.0 equiv) in DMF were stirred at room temperature for 2 h. The mixture was diluted with water, and the precipitate was collected by filtration, washed with water and dried under vacuum to give **11a** or **11b**.

4.1.1.6. General procedure for the preparation of 11c. To a stirred solution of **10** (1.0 equiv) and 4-dimethylaminopyridine (DMAP, 0.2 equiv) in CH$_2$Cl$_2$ at 0 °C was added drop-wise acetyl chloride (1.1 equiv). The resulting suspension was allowed to warm to ambient temperature and then stirred for 30 min. The reaction was then diluted with CH$_2$Cl$_2$, washed with saturated

NaHCO$_3$ and water, dried over MgSO$_4$ and then purified by silica gel chromatography to give **11c**.

4.1.2. General procedure for the preparation of compounds 15a–15h and 16a–16t

Compound **12** (1.0 equiv) was suspended in EtOH/H$_2$O (v/v: 3:1), and iron powder (10.0 equiv) and NH$_4$Cl (3.0 equiv) were added. The suspension was heated to reflux for 1 h with vigorous stirring. The precipitate was separated by filtration and washing with ethanol. The filtrates were evaporated and the resulting oil was added to cold saturated NaHCO$_3$ followed by extracted with acetic ether. The combined organic layers were dried (MgSO$_4$), filtered and the filtrate was concentrated under reduced pressure. The crude amide (**13**) was used for the next reaction without further purification. A solution of **13** (1.0 equiv) and **14** (1.0 equiv) in chloroform was heated at 60 °C for 2 h. The reaction mixture was purified by silica gel chromatography to give **15a–15h** and **16a–16t** as solid.
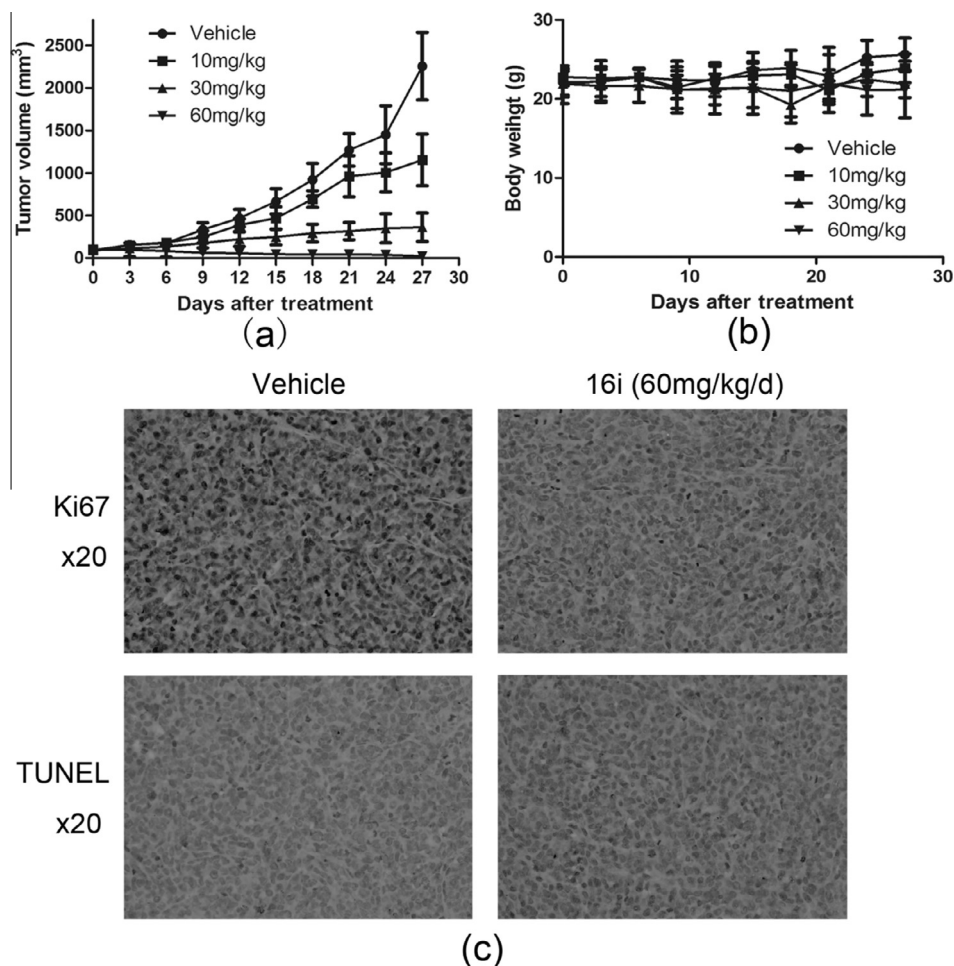
Figure 5. (a) Antitumor efficacy of **16i** at concentrations of 10, 30, and 60 mg/kg/d in an in vivo MV4-11 xenograft model. (b) Average body weights for **16i**-treated mice groups at different doses and vehicle group in an in vivo MV4-11 xenograft model. (c) Ki67 and TUNEL staining of tumor tissues showing the inhibition of cell proliferation and the induction of apoptosis.

4.1.2.1. *N*-(5-(*tert*-Butyl)isoxazol-3-yl)-*N'*-(4-(imidazo[1,2-*a*]pyridin-2-yl)phenyl)urea (15a). Overall yield: 14.5%. ^{1}H NMR (400 MHz, DMSO-d_6) δ 9.56 (s, 1H), 8.92 (s, 1H), 8.50 (d, $J = 6.6$ Hz, 1H), 8.32 (s, 1H), 7.92 (d, $J = 7.8$ Hz, 2H), 7.56 (d, $J = 7.5$ Hz, 2H), 7.52 (d, $J = 6.7$ Hz, 1H), 7.22 (t, $J = 7.8$ Hz, 1H), 6.87 (t, $J = 6.5$ Hz, 1H), 6.54 (s, 1H), 1.30 (s, 9H); ^{13}C NMR (101 MHz, DMSO-d_6) δ 180.16, 158.36, 151.27, 144.74, 144.29, 138.49, 128.29, 126.70, 126.15, 124.68, 118.59, 116.41; MS (ES$^+$) m/z calcd for $C_{21}H_{21}N_5O_2$: 375.17; found: 376.2 (M+H$^+$).

4.1.2.2. *N*-(5-(*tert*-Butyl)isoxazol-3-yl)-*N'*-(4-(imidazo[1,2-*a*]pyrimidin-2-yl)phenyl)urea (15b). Overall yield: 7.2%. ^{1}H NMR (400 MHz, DMSO-d_6) δ 10.34 (s, 1H), 10.03 (s, 1H), 9.32 (d, $J = 6.1$ Hz, 1H), 8.96 (d, $J = 5.8$ Hz, 1H), 8.69 (s, 1H), 7.96 (d, $J = 7.9$ Hz, 2H), 7.66 (d, $J = 8.0$ Hz, 2H), 7.64 (t, $J = 6.5$ Hz, 1H), 6.53 (s, 1H), 1.30 (s, 9H); ^{13}C NMR (101 MHz, DMSO-d_6) δ 180.10, 158.04, 156.13, 151.45, 144.20, 141.39, 137.41, 136.38, 127.16, 120.00, 118.20, 113.61, 108.36, 92.48, 32.43, 28.34; MS (ES$^+$) m/z calcd for $C_{20}H_{20}N_6O_2$: 376.16; found: 377.2 (M+H$^+$).

4.1.2.3. *N*-(5-(*tert*-butyl)Isoxazol-3-yl)-*N'*-(4-(imidazo[1,2-*a*]pyrazin-2-yl)phenyl)urea (15c). Overall yield: 11.6%. ^{1}H NMR (400 MHz, DMSO-d_6) δ 9.58 (s, 1H), 9.05 (s, 1H), 8.99 (s, 1H), 8.58 (d, $J = 6.5$ Hz, 1H), 8.53 (s, 1H), 7.98 (d, $J = 7.9$ Hz, 2H), 7.89 (d, $J = 6.3$ Hz, 1H), 7.58 (d, $J = 8.2$ Hz, 2H), 6.53 (s, 1H), 1.31 (s, 9H); ^{13}C NMR (101 MHz, DMSO-d_6) δ 180.21, 158.31, 151.25, 144.74,

142.26, 140.32, 129.11, 127.38, 126.65, 119.92, 118.60, 109.86, 98.36, 92.44, 32.46. 28.22; MS (ES$^+$) m/z calcd for $C_{20}H_{20}N_6O_2$: 376.16; found: 399.2 (M+Na$^+$).

4.1.2.4. *N*-(5-(*tert*-Butyl)isoxazol-3-yl)-*N'*-(4-(imidazo[1,2-*b*]pyridazin-2-yl)phenyl)urea (15d). Overall yield: 12.3%. ^{1}H NMR (400 MHz, DMSO-d_6) δ 9.64 (s, 1H), 9.16 (s, 1H), 8.77 (s, 1H), 8.47 (d, $J = 8.3$ Hz, 1H), 8.09 (d, $J = 8.1$ Hz, 1H), 7.99 (d, $J = 7.1$ Hz, 2H), 7.57 (d, $J = 7.1$ Hz, 2H), 7.21 (t, $J = 8.5$ Hz, 1H), 6.54 (s, 1H), 1.29 (s, 9H); ^{13}C NMR (101 MHz, DMSO-d_6) δ 180.16, 158.31, 151.31, 144.55, 143.56, 139.06, 138.83, 127.55, 126.30, 124.68, 118.49, 117.45, 112.39, 92.45, 32.43, 28.31; MS (ES$^+$) m/z calcd for $C_{20}H_{20}N_6O_2$: 376.16; found: 377.2 (M+H$^+$).

4.1.2.5. *N*-(4-(Benzo[*b*]thiophen-2-yl)phenyl)-*N'*-(5-(*tert*-butyl)isoxazol-3-yl)urea (15e). Overall yield: 8.5%. ^{1}H NMR (400 MHz, DMSO-d_6) δ 9.60 (s, 2H), 7.94 (d, $J = 7.7$ Hz, 1H), 7.81 (d, $J = 7.6$ Hz, 1H), 7.76 (s, 1H), 7.72 (d, $J = 8.0$ Hz, 2H), 7.60 (d, $J = 8.0$ Hz, 2H), 7.38 (d, $J = 7.8$ Hz, 1H), 7.33 (d, $J = 8.0$ Hz, 1H), 6.54 (s, 1H), 1.30 (s, 9H); ^{13}C NMR (101 MHz, DMSO-d_6) δ 180.04, 158.53, 151.51, 143.19, 140.61, 139.63, 138.22, 127.48, 126.63, 124.71, 124.29, 123.42, 122.33, 118.76, 92.57, 32.43, 28.34; MS (ES$^+$) m/z calcd for $C_{21}H_{20}N_3O_2S$: 391.14; found: 414.2 (M+Na$^+$).

4.1.2.6. *N*-(4-(Benzofuran-2-yl)phenyl)-*N'*-(5-(*tert*-butyl)isoxazol-3-yl)urea (15f). Overall yield: 10.8%. ^{1}H NMR (400 MHz,

DMSO-d_6) δ 9.61 (s, 1H), 9.06 (s, 1H), 7.86 (d, J = 6.0 Hz, 2H), 7.62 (s, 4H), 7.29 (d, J = 6.2 Hz, 2H), 7.25 (s, 1H), 6.54 (s, 1H), 1.30 (s, 9H); ^{13}C NMR (101 MHz, DMSO-d_6) δ 180.23, 158.27, 155.24, 154.02, 151.22, 139.56, 129.00, 125.46, 124.14, 123.91, 123.12, 120.83, 118.62, 110.91, 100.58, 92.46, 32.45, 28.31; MS (ES$^+$) m/z calcd for $C_{22}H_{21}N_3O_3$: 375.16; found: 398.2 (M+Na$^+$).

4.1.2.7. **N-(4-(Benzo[d]oxazol-2-yl)phenyl)-N'-(5-(*tert*-butyl)isoxazol-3-yl)urea (15g).** Overall yield: 4.8%. ^{1}H NMR (400 MHz, DMSO-d_6) δ 9.65 (s, 1H), 9.19 (s, 1H), 8.12 (d, J = 7.7 Hz, 1H), 8.06 (d, J = 7.8 Hz, 2H), 8.02 (d, J = 7.5 Hz, 1H), 7.67 (d, J = 7.9 Hz, 2H), 7.54 (t, J = 7.2 Hz, 1H), 7.44 (t, J = 7.2 Hz, 1H), 6.55 (s, 1H), 1.31 (s, 9H); ^{13}C NMR (101 MHz, DMSO-d_6) δ 180.31, 166.95, 158.19, 153.62, 151.15, 141.92, 134.20, 128.13, 126.87, 126.54, 125.18, 122.50, 122.21, 118.55, 92.48, 32.47, 28.32; MS (ES$^+$) m/z calcd for $C_{21}H_{20}N_4O_2$: 376.15; found: 377.2 (M+H$^+$).

4.1.2.8. **N-(4-(Benzo[d]thiazol-2-yl)phenyl)-N'-(5-(*tert*-butyl)isoxazol-3-yl)urea (15h).** Overall yield: 5.7%. ^{1}H NMR (400 MHz, DMSO-d_6) δ 9.67 (s, 1H), 9.21 (s, 1H), 8.15 (d, J = 7.8 Hz, 2H), 7.77 (d, J = 4.1 Hz, 2H), 7.71 (d, J = 7.8 Hz, 2H), 7.40 (d, J = 4.0 Hz, 2H), 6.55 (s, 1H), 1.31 (s, 9H); ^{13}C NMR (101 MHz, DMSO-d_6) δ 162.24, 158.17, 151.16, 150.08, 142.40, 141.63, 128.35, 125.09, 124.74, 120.09, 119.46, 118.47, 110.71, 99.49, 92.48, 32.47, 28.32; MS (ES$^+$) m/z calcd for $C_{21}H_{20}N_4O_2S$: 392.13; found: 393.1 (M+H$^+$).

4.1.2.9. **N-(5-(*tert*-Butyl)isoxazol-3-yl)-N'-(4-(8-fluoroimidazo[1,2-a]pyridin-2-yl)phenyl)urea (16a).** Overall yield: 5.5%. ^{1}H NMR (400 MHz, DMSO-d_6) δ 9.56 (s, 1H), 8.95 (s, 1H), 8.74 (s, 1H), 8.32 (s, 1H), 7.90 (d, J = 8.2 Hz, 2H), 7.62 (m, 1H), 7.54 (d, J = 8.2 Hz, 2H), 7.31 (t, J = 9.0 Hz, 1H), 6.53 (s, 1H), 1.30 (s, 9H); ^{13}C NMR (100 MHz, DMSO-d_6) δ 180.17, 158.33, 152.47 (d, J = 230.2 Hz), 151.26, 145.56, 142.65, 138.66, 127.92, 126.16, 118.57, 117.02 (d, J = 9.4 Hz), 116.37 (d, J = 26.5 Hz), 113.42 (d, J = 41.4 Hz), 109.88, 92.43, 32.44, 28.31; MS (ES$^+$) m/z calcd for $C_{21}H_{20}FN_5O_2$: 393.16; found: 394.2 (M+H$^+$).

4.1.2.10. **N-(5-(*tert*-Butyl)isoxazol-3-yl)-N'-(4-(8-chloroimidazo[1,2-a]pyridin-2-yl)phenyl)urea (16b).** Overall yield: 15.1%. ^{1}H NMR (400 MHz, DMSO-d_6) δ 9.55 (s, 1H), 8.91 (s, 1H), 8.31 (s, 1H), 8.18 (s, 1H), 7.88 (d, J = 8.0 Hz, 2H), 7.53 (d, J = 7.9 Hz, 2H), 7.45 (d, J = 9.2 Hz, 1H), 6.96 (d, J = 9.2 Hz, 1H), 6.53 (s, 1H), 1.30 (s, 9H); ^{13}C NMR (101 MHz, DMSO-d_6) δ 180.16, 158.36, 151.26, 144.16, 143.90, 138.36, 128.39, 127.43, 126.02, 124.19, 122.67, 118.56, 116.00, 108.00, 92.42, 32.44, 28.31; MS (ES$^+$) m/z calcd for $C_{21}H_{20}ClN_5O_2$: 409.13; found: 410.2 (M+H$^+$).

4.1.2.11. **N-(5-(*tert*-Butyl)isoxazol-3-yl)-N'-(4-(8-methylimidazo[1,2-a]pyridin-2-yl)phenyl)urea (16c).** Overall yield: 11.9%. ^{1}H NMR (400 MHz, DMSO-d_6) δ 9.55 (s, 1H), 8.95 (s, 1H), 8.33 (d, J = 6.6 Hz, 1H), 8.29 (s, 1H), 7.92 (d, J = 6.8 Hz, 2H), 7.55 (d, J = 6.9 Hz, 2H), 7.01 (d, J = 6.7 Hz, 1H), 6.77 (t, J = 7.2 Hz, 1H), 6.54 (s, 1H), 2.53 (s, 3H), 1.30 (s, 9H); ^{13}C NMR (101 MHz, DMSO-d_6) δ 180.19, 158.36, 151.27, 145.21, 143.63, 138.36, 128.41, 126.13, 125.92, 124.42, 123.21, 118.57, 112.02, 108.79, 92.44, 32.43, 28.30, 16.66; MS (ES$^+$) m/z calcd for $C_{22}H_{23}N_5O_2$: 389.19; found: 390.2 (M+H$^+$).

4.1.2.12. **N-(5-(*tert*-Butyl)isoxazol-3-yl)-N'-(4-(8-(trifluoromethyl)imidazo[1,2-a]pyridin-2-yl)phenyl)urea (16d).** Overall yield: 9.9%. ^{1}H NMR (400 MHz, DMSO-d_6) δ 9.55 (s, 1H), 8.97 (s, 1H), 8.79 (d, J = 5.5 Hz, 1H), 8.51 (s, 1H), 7.94 (d, J = 7.4 Hz, 2H), 7.69 (d, J = 5.8 Hz, 1H), 7.57 (d, J = 7.5 Hz, 2H), 7.02 (t, J = 7.8 Hz, 1H), 6.54 (s, 1H), 1.30 (s, 9H); ^{13}C NMR (101 MHz, DMSO-d_6) δ 180.19,

158.33, 151.23, 145.12, 139.84, 138.98, 130.80, 127.36, 126.50, 123.76 (q, J = 4.2 Hz), 123.09 (q, J = 270.8 Hz), 118.56, 116.33 (q, J = 32.0 Hz), 110.63, 109.61, 92.44, 32.44, 28.31; MS (ES$^+$) m/z calcd for $C_{22}H_{20}F_3N_5O_2$: 443.16; found: 444.2 (M+H$^+$).

4.1.2.13. **N-(5-(*tert*-Butyl)isoxazol-3-yl)-N'-(4-(7-chloroimidazo[1,2-a]pyridin-2-yl)phenyl)urea (16e).** Overall yield: 13.9%. ^{1}H NMR (400 MHz, DMSO-d_6) δ 9.81 (s, 1H), 9.63 (s, 1H), 8.83 (d, J = 7.1 Hz, 1H), 8.65 (s, 1H), 8.01 (s, 1H), 7.92 (d, J = 8.2 Hz, 2H), 7.66 (d, J = 8.2 Hz, 2H), 7.48 (d, J = 6.8 Hz, 1H), 6.53 (s, 1H), 1.30 (s, 9H); ^{13}C NMR (101 MHz, DMSO-d_6) δ 180.21, 158.16, 151.36, 144.49, 141.11, 140.77, 129.53, 127.43, 126.94, 124.37, 118.57, 111.94, 110.13, 108.00, 92.47, 32.46, 28.33; MS (ES$^+$) m/z calcd for $C_{21}H_{20}ClN_5O_2$: 409.13; found: 410.1 (M+H$^+$).

4.1.2.14. **N-(5-(*tert*-Butyl)isoxazol-3-yl)-N'-(4-(7-bromoimidazo[1,2-a]pyridin-2-yl)phenyl)urea (16f).** Overall yield: 16.1%. ^{1}H NMR (400 MHz, DMSO-d_6) δ 10.03 (s, 1H), 9.95 (s, 1H), 8.73 (s, 1H), 8.63 (d, J = 6.3 Hz, 1H), 7.96 (d, J = 8.1 Hz, 2H), 7.66 (s, 1H), 7.64 (d, J = 8.0 Hz, 2H), 7.27 (d, J = 5.8 Hz, 1H), 6.54 (s, 1H), 1.30 (s, 9H); ^{13}C NMR (101 MHz, DMSO-d_6) δ 180.11, 158.14, 151.46, 144.49, 141.11, 140.59, 129.53, 127.05, 126.94, 124.37, 118.29, 111.13, 110.13, 108.00, 92.47, 32.44, 28.34; MS (ES$^+$) m/z calcd for $C_{21}H_{20}BrN_5O_2$: 453.08; found: 454.1 (M+H$^+$).

4.1.2.15. **N-(5-(*tert*-Butyl)isoxazol-3-yl)-N'-(4-(7-methylimidazo[1,2-a]pyridin-2-yl)phenyl)urea (16g).** Overall yield: 12.8%. ^{1}H NMR (400 MHz, DMSO-d_6) δ 9.57 (s, 1H), 8.97 (s, 1H), 8.37 (d, J = 7.1 Hz, 1H), 8.21 (s, 1H), 7.88 (d, J = 8.2 Hz, 2H), 7.53 (d, J = 8.2 Hz, 2H), 7.32 (s, 1H), 6.71 (d, J = 6.8 Hz, 1H), 6.53 (s, 1H), 2.34 (s, 3H), 1.29 (s, 9H); ^{13}C NMR (101 MHz, DMSO-d_6) δ 180.15, 158.35, 151.28, 145.12, 143.96, 138.34, 135.15, 128.39, 126.03, 125.90, 118.54, 114.66, 114.55, 107.70, 92.43, 32.43, 28.31, 20.78; MS (ES$^+$) m/z calcd for $C_{22}H_{23}N_5O_2$: 389.19; found: 390.2 (M+H$^+$).

4.1.2.16. **N-(5-(*tert*-Butyl)isoxazol-3-yl)-N'-(4-(7-ethynylimidazo[1,2-a]pyridin-2-yl)phenyl)urea (16h).** Overall yield: 15.5%. ^{1}H NMR (400 MHz, DMSO-d_6) δ 9.83 (s, 1H), 9.68 (s, 1H), 8.74 (d, J = 6.3 Hz, 1H), 8.64 (s, 1H), 8.13 (s, 1H), 7.93 (d, J = 7.9 Hz, 2H), 7.66 (d, J = 8.1 Hz, 2H), 7.56 (d, J = 6.1 Hz, 1H), 6.53 (s, 1H), 3.07 (s, 1H), 1.30 (s, 9H); ^{13}C NMR (101 MHz, DMSO-d_6) δ 180.20, 179.74, 158.16(s), 152.86, 151.37, 146.41, 140.72, 136.53, 126.94, 122.07, 118.54, 116.87, 110.12, 106.02, 92.47, 80.47, 75.32, 32.45, 28.34; MS (ES$^+$) m/z calcd for $C_{23}H_{21}N_5O_2$: 399.17; found: 400.3 (M+H$^+$).

4.1.2.17. **N-(5-(*tert*-Butyl)isoxazol-3-yl)-N'-(4-(7-methoxyimidazo[1,2-a]pyridin-2-yl)phenyl)urea (16i).** Overall yield: 9.6%. ^{1}H NMR (400 MHz, DMSO-d_6) δ 9.54 (s, 1H), 8.91 (s, 1H), 8.36 (d, J = 7.1 Hz, 1H), 8.11 (s, 1H), 7.85 (d, J = 7.9 Hz, 2H), 7.52 (d, J = 8.0 Hz, 2H), 6.95 (s, 1H), 6.60 (d, J = 7.0 Hz, 1H), 6.53 (s, 1H), 3.84 (s, 3H), 1.30 (s, 9H); ^{13}C NMR (101 MHz, DMSO-d_6) δ 180.16, 158.36, 157.34, 151.27, 146.16, 143.85, 138.17, 128.53, 127.24, 125.86, 118.57, 106.98, 106.56, 94.20, 92.42, 55.49, 32.44, 28.32; MS (ES$^+$) m/z calcd for $C_{22}H_{23}N_5O_3$: 405.18; found: 406.2 (M+H$^+$).

4.1.2.18. **N-(5-(*tert*-Butyl)isoxazol-3-yl)-N'-(4-(7-ethoxyimidazo[1,2-a]pyridin-2-yl)phenyl)urea (16j).** Overall yield: 7.1%. ^{1}H NMR (400 MHz, DMSO-d_6) δ 9.55 (s, 1H), 8.90 (s, 1H), 8.35 (d, J = 7.2 Hz, 1H), 8.11 (s, 1H), 7.84 (d, J = 8.0 Hz, 2H), 7.51 (d, J = 8.1 Hz, 2H), 6.92 (s, 1H), 6.59 (d, J = 7.2 Hz, 1H), 6.53 (s, 1H), 4.10 (q, J = 8.1 Hz, 2H), 1.37 (t, J = 6.4 Hz, 3H), 1.30 (s, 9H); ^{13}C NMR (101 MHz, DMSO-d_6) δ 180.16, 158.35, 156.51, 151.26, 146.14, 143.76, 138.17, 128.48, 127.27, 125.84, 118.56, 106.95,

106.76, 94.65, 92.42, 63.55, 32.45, 28.33, 14.28; MS (ES$^+$) m/z calcd for $C_{23}H_{22}N_5O_3$: 419.20; found: 420.3 (M+H$^+$).

4.1.2.19. 2-(4-(3-(5-(tert-Butyl)isoxazol-3-yl)ureido)phenyl)imidazo[1,2-a]pyridin-7-yl acetate (16k).
Overall yield: 6.3%. ^{1}H NMR (400 MHz, DMSO-d_6) δ 9.56 (s, 1H), 8.96 (s, 1H), 8.55 (d, J = 7.9 Hz, 1H), 8.33 (s, 1H), 7.89 (d, J = 7.3 Hz, 2H), 7.54 (d, J = 7.7 Hz, 2H), 7.35 (s, 1H), 6.81 (d, J = 7.6 Hz, 1H), 6.53 (s, 1H), 2.32 (s, 3H), 1.31 (s, 9H); ^{13}C NMR (101 MHz, DMSO-d_6) δ 180.18, 169.39, 158.34, 151.25, 145.24, 143.13, 138.79, 138.62, 126.17, 125.85, 121.87, 119.43, 118.58, 116.20, 109.37, 92.43, 32.45, 28.42, 28.33; MS (ES$^+$) m/z calcd for $C_{23}H_{23}N_5O_4$: 433.18; found: 434.2 (M+H$^+$).

4.1.2.20. N-(5-(tert-Butyl)isoxazol-3-yl)-N′-(4-(6-fluoroimidazo[1,2-a]pyridin-2-yl)phenyl)urea (16l).
Overall yield: 7.2%. ^{1}H NMR (400 MHz, DMSO-d_6) δ 9.61 (s, 1H), 9.08 (s, 1H), 8.52 (d, J = 6.3 Hz, 1H), 8.45 (s, 1H), 7.93 (d, J = 7.8 Hz, 2H), 7.57 (d, J = 7.8 Hz, 2H), 7.41 (s, 1H), 6.87 (d, J = 6.6 Hz, 1H), 6.54 (s, 1H), 1.30 (s, 9H); ^{13}C NMR (101 MHz, DMSO-d_6) δ 180.16, 158.33, 151.28 (d, J = 24.2 Hz), 144.64, 141.86, 138.86, 127.57, 126.33, 125.96, 123.89, 120.91 (d, J = 43.4 Hz), 118.53 (d, J = 240.8 Hz), 111.91 (d, J = 39.8 Hz), 110.32, 92.45, 32.43, 28.31; MS (ES$^+$) m/z calcd for $C_{21}H_{20}FN_5O_2$: 393.16; found: 394.2 (M+H$^+$).

4.1.2.21. N-(5-(tert-Butyl)isoxazol-3-yl)-N′-(4-(6-chloroimidazo[1,2-a]pyridin-2-yl)phenyl)urea (16m).
Overall yield: 12.6%. ^{1}H NMR (400 MHz, DMSO-d_6) δ 8.96 (s, 1H), 8.80 (s, 1H), 8.30 (s, 1H), 7.91 (d, J = 7.5 Hz, 2H), 7.61 (d, J = 9.3 Hz, 1H), 7.55 (d, J = 7.5 Hz, 2H), 7.28 (d, J = 9.3 Hz, 1H), 6.54 (s, 1H), 1.31 (s, 9H); ^{13}C NMR (101 MHz, DMSO-d_6) δ 180.18, 158.33, 151.25, 145.30, 143.21, 138.78, 127.71, 126.26, 125.50, 124.62, 118.79, 118.58, 117.15, 109.00, 92.43, 32.44, 28.32; MS (ES$^+$) m/z calcd for $C_{21}H_{20}ClN_5O_2$: 409.13; found: 410.2 (M+H$^+$).

4.1.2.22. N-(5-(tert-Butyl)isoxazol-3-yl)-N′-(4-(6-bromoimidazo[1,2-a]pyridin-2-yl)phenyl)urea (16n).
Overall yield: 12.8%. ^{1}H NMR (400 MHz, DMSO-d_6) δ 9.60 (s, 1H), 9.06 (s, 1H), 8.86 (s, 1H), 8.29 (s, 1H), 7.90 (d, J = 8.0 Hz, 2H), 7.55 (d, J = 8.3 Hz, 2H), 7.50 (d, J = 9.0 Hz, 1H), 7.34 (d, J = 9.4 Hz, 1H), 6.53 (s, 1H), 1.30 (s, 9H); ^{13}C NMR (101 MHz, DMSO-d_6) δ 180.16, 158.32, 151.28, 145.09, 143.25, 138.82, 127.65, 127.58, 126.70, 126.271 118.54, 117.42, 108.78, 105.72, 92.44, 32.44, 28.33; MS (ES$^+$) m/z calcd for $C_{21}H_{20}BrN_5O_2$: 453.08; found: 454.1 (M+H$^+$).

4.1.2.23. N-(5-(tert-Butyl)isoxazol-3-yl)-N′-(4-(6-iodoimidazo[1,2-a]pyridin-2-yl)phenyl)urea (16o).
Overall yield: 9.5%. ^{1}H NMR (400 MHz, DMSO-d_6) δ 9.92 (s, 1H), 9.88 (s, 1H), 9.21 (s, 1H), 8.55 (s, 1H), 8.04 (d, J = 8.7 Hz, 1H), 7.90 (d, J = 7.4 Hz, 2H), 7.73 (d, J = 8.8 Hz, 1H), 7.63 (d, J = 7.7 Hz, 2H), 6.52 (s, 1H), 1.30 (s, 9H); ^{13}C NMR (101 MHz, DMSO-d_6) δ 180.15, 158.08, 151.35, 141.12, 139.69, 139.13, 136.00, 132.95, 127.06, 119.96, 118.34, 113.08, 109.47, 92.48, 81.53, 32.44, 28.34; MS (ES$^+$) m/z calcd for $C_{21}H_{20}IN_5O_2$: 501.07; found: 502.1 (M+H$^+$).

4.1.2.24. N-(5-(tert-Butyl)isoxazol-3-yl)-N′-(4-(6-methylimidazo[1,2-a]pyridin-2-yl)phenyl)urea (16p).
Overall yield: 18.4%. ^{1}H NMR (400 MHz, DMSO-d_6) δ 9.88 (s, 1H), 9.82 (s, 1H), 8.68 (s, 1H), 8.63 (s, 1H), 7.93 (d, J = 8.3 Hz, 2H), 7.86 (d, J = 9.1 Hz, 1H), 7.79 (d, J = 9.1 Hz, 1H), 7.67 (d, J = 8.2 Hz, 2H), 6.54 (s, 1H), 2.42 (s, 3H), 1.31 (s, 9H); ^{13}C NMR (101 MHz, DMSO-d_6) δ 180.20, 158.12, 151.38, 143.27, 141.02, 138.73, 135.45, 135.40, 126.96, 126.33, 120.14, 118.45, 111.21, 109.80, 92.47, 32.46, 28.33, 17.37; MS (ES$^+$) m/z calcd for $C_{22}H_{23}N_5O_2$: 389.19; found: 390.2 (M+H$^+$).

4.1.2.25. N-(5-(tert-Butyl)isoxazol-3-yl)-N′-(4-(6-ethynylimidazo[1,2-a]pyridin-2-yl)phenyl)urea (16q).
Overall yield: 12.1%. ^{1}H NMR (400 MHz, DMSO-d_6) δ 9.33 (s, 1H), 8.74 (s, 1H), 8.56 (d, J = 6.2 Hz, 1H), 8.05 (d, J = 6.0 Hz, 1H), 7.66 (d, J = 8.2 Hz, 2H), 7.31 (d, J = 8.0 Hz, 2H), 7.27 (s, 1H), 7.00 (s, 1H), 6.29 (s, 1H), 4.02 (s, 1H), 1.05 (s, 9H); ^{13}C NMR (101 MHz, DMSO-d_6) δ 180.19, 158.33, 151.26, 145.23, 143.66, 138.80, 130.35, 127.66, 127.07, 126.28, 118.59, 116.45, 108.76, 106.75, 92.43, 81.62, 80.21, 32.43, 28.30; MS (ES$^+$) m/z calcd for $C_{23}H_{21}N_5O_2$: 399.17; found: 400.2 (M+H$^+$).

4.1.2.26. N-(5-(tert-Butyl)isoxazol-3-yl)-N′-(4-(6-cyclopropylimidazo[1,2-a]pyridin-2-yl)phenyl)urea (16r).
Overall yield: 12.6% ^{1}H NMR (400 MHz, DMSO-d_6) δ 9.52 (s, 1H), 8.89 (s, 1H), 8.32 (s, 1H), 8.18 (s, 1H), 7.87 (d, J = 8.1 Hz, 2H), 7.52 (d, J = 8.1 Hz, 2H), 7.45 (d, J = 9.2 Hz, 1H), 6.97 (d, J = 9.3 Hz, 1H), 6.52 (s, 1H), 2.04–1.88 (m, 1H), 1.30 (s, 9H), 0.94 (m, 2H), 0.71 (m, 2H); ^{13}C NMR (101 MHz, DMSO-d_6) δ 180.17, 158.34, 151.24, 144.12, 143.89, 138.34, 128.37, 127.45, 126.02, 124.21, 122.67, 118.54, 116.00, 108.02, 92.42, 32.45, 28.32, 12.37, 7.65; MS (ES$^+$) m/z calcd for $C_{24}H_{25}N_5O_2$: 415.20; found: 416.3 (M+H$^+$).

4.1.2.27. N-(5-(tert-Butyl)isoxazol-3-yl)-N′-(4-(5-chloroimidazo[1,2-a]pyridin-2-yl)phenyl)urea (16s).
Overall yield: 8.5%. ^{1}H NMR (400 MHz, DMSO-d_6) δ 9.99 (s, 1H), 9.93 (s, 1H), 8.89 (s, 1H), 8.07 (d, J = 8.0 Hz, 2H), 7.94 (d, J = 8.1 Hz, 1H), 7.86 (t, J = 8.0 Hz, 1H), 7.69 (d, J = 7.8 Hz, 1H), 7.63 (d, J = 8.0 Hz, 2H), 6.55 (s, 1H), 1.31 (s, 9H); ^{13}C NMR (101 MHz, DMSO-d_6) δ 180.15, 158.09, 151.38, 141.63, 141.14, 136.95, 132.48, 127.93, 127.22, 120.30, 118.18, 116.70, 111.05, 108.59, 92.48, 32.44, 28.33; MS (ES$^+$) m/z calcd for $C_{21}H_{20}ClN_5O_2$: 409.13; found: 410.2 (M+H$^+$).

4.1.2.28. N-(5-(tert-Butyl)isoxazol-3-yl)-N′-(4-(5-methylimidazo[1,2-a]pyridin-2-yl)phenyl)urea (16t).
Overall yield: 7.1%. ^{1}H NMR (400 MHz, DMSO-d_6) δ 9.57 (s, 1H), 8.93 (s, 1H), 8.28 (s, 1H), 7.98 (d, J = 6.2 Hz, 2H), 7.54 (d, J = 6.4 Hz, 2H), 7.46 (d, J = 7.8 Hz, 1H), 7.21 (t, J = 7.6 Hz, 1H), 6.76 (d, J = 7.8 Hz, 1H), 6.54 (s, 1H), 2.63 (s, 3H), 1.30 (s, 9H); ^{13}C NMR (101 MHz, DMSO-d_6) δ 180.16, 158.37, 151.27, 145.13, 144.25, 138.49, 135.09, 126.20, 124.83, 118.51, 113.79, 111.10, 106.17, 99.48, 92.45, 32.44, 28.31, 18.29; MS (ES$^+$) m/z calcd for $C_{22}H_{23}N_5O_2$: 389.19; found: 390.2 (M+H$^+$).

4.2. Kinase inhibitory assays

The kinase inhibitory assays were performed according to the KinaseProfiler assay protocols of Upstate Biotechnology (Millipore).

4.3. Cell culture and cell viability assays

All cell lines were obtained from the American Type Culture Collection (Manassas, VA, USA). Cells were maintained in RPMI 1640 or DMEM medium supplemented with 10% FBS (v/v) in 5% CO_2 at 37 °C, except for MV4-11 cells, which were cultured in IMDM medium. The leukemia cells were seeded in a 96-well plate at $1–4 \times 10^4$ cells per well, and an equal volume of medium containing increasing concentrations of inhibitors was added to each well. At the end of the incubation period (72 h at 37 °C), 20 µL of 5 mg/mL MTT reagent was added per well for 2–4 h, and 50 µL of 20% SDS (w/v) per well was used to dissolve the cells. The other cell lines were seeded in 96-well plates at a density of $2–5 \times 10^3$ cells/well. After incubation for 24 h in serum-containing media, the cells were treated with inhibitors diluted with culture medium for 72 h at 37 °C under a 5% CO_2 atmosphere. Thereafter, the MTT reagent was added for 2–4 h, and DMSO was used to dissolve the

Y. Xu et al./Bioorg. Med. Chem. 23 (2015) 4333–4343

4343

cells. Finally, the light absorption (OD) of the dissolved cells was measured at 570 nM using a Multiskan MK3 ELISA photometer (Thermo Scientific).

4.4. Pharmacokinetic analysis

Female Sprague–Dawley rats (200–250 g) were used and randomly divided into two groups ($n = 3$ in each group). A catheter was surgically placed into the femoral vein for collection of blood samples. Rats were fasted overnight before dosing. Compounds **16i** was administered orally (po) by gavage at 30 mg/kg in 25% PEG400, 5% DMSO (Sigma–Aldrich) and 70% distilled water. Blood was collected into heparin-containing tubes for plasma at 15 min, 30 min, 1 h, 2 h, 4 h, 6 h, 12 h and 24 h postdose, and the plasma was isolated by centrifugation. Plasma concentrations of each compound were determined using liquid–liquid extraction followed by HPLC (an UltiMate 3000 HPLC system, Dionex, USA).

4.5. Western blot analysis

After treatment with compound **16i** for 2 h at 37 °C, MV4-11 cells were harvested, washed with ice-cold PBS, and suspended in RIPA lysis buffer (Beyotime) including 1% cocktail (Sigma–Aldrich). Cell lysates were centrifuged for 15 min at 13,000 rpm and 4 °C to remove any insoluble material. Proteins were separated by gel electrophoresis on 5–10% polyacrylamide gels and transferred onto PVDF membranes (Millipore). The PVDF membranes were incubated with the anti-FLT3, anti-p-FLT3 and anti-β-actin antibody, washed with TBST buffer and blotted with horseradish peroxidase-conjugated secondary antibody. Finally, the membranes were developed with SuperSignal reagent (Pierce, Rockford, IL, USA) upon exposure to X-ray film.

4.6. Apoptosis analysis in MV4-11 cells

A total of 4×10^5 MV4-11 cells were seeded in a six-well plate and treated with compound **16i** for 48 h at 37 °C. After incubation, the cells were harvested and washed with PBS. The apoptosis ratio was analyzed using an Annexin V-FITC Apoptosis Analysis Kit (TianJin Suangene Biotech Co.) and BD FACSCalibur.

4.7. In vivo model

MV4-11 cells were harvested during the exponential-growth phase, washed three times with serum-free medium, and resuspension at a concentration of 1×10^8 cell/mL. Tumor xenograft models were established by subcutaneously injecting 100 μL of cell suspension into NOD-SCID mice (5–6 weeks). When the tumors had grown to 100–200 mm³, the mice were randomized into 4 groups (6 mice for each group) and treated with **16i** (10, 30, or 60 mg/kg/d) or vehicle alone (25% PEG400 plus 5% DMSO in distilled water) via oral gavage. Tumor growth was measured twice weekly using Vernier calipers and the volume was calculated as follows: tumor size = $a \times b^2 \times 0.5$ (a = long diameter; b = short diameter).

4.8. Immunohistochemistry

NOD-SCID mice bearing tumors were treated with **16i** (60 mg/kg/d) via oral gavage, and the tumors were harvested 7 days later. The tumors were fixed with formalin and embedded in paraffin. Sections measuring 4–8 μm in thickness were prepared for immunohistochemical analysis. Proliferation was detected using immunostaining with the Ki67 antibody (Thermo Fisher Scientific, Fremont, CA). Apoptosis was determined using transferase-mediated dUTP nick-end labeling (TUNEL) and staining (Roche Applied Science). Finally, images were captured with an Olympus digital camera attached to a light microscope.

References and notes

1. Rosnet, O.; Marchetto, S.; DeLapeyriere, O.; Birnbaum, D. *Oncogene* **1991**, *6*, 1641.
2. Rosnet, O.; Bühring, H.-J.; Beslu, N.; Lavagna, C.; Marchetto, S.; Rappold, I.; Drexler, H. G.; Birg, F.; Rottapel, R.; Hannum, C. *Acta Haematol.* **1996**, *95*, 218.
3. Rosnet, O.; Schiff, C.; Pebusque, M. J.; Marchetto, S.; Tonnelle, C.; Toiron, Y.; Birg, F.; Birnbaum, D. *Blood* **1993**, *82*, 1110.
4. Mackarehtschian, K.; Hardin, J. D.; Moore, K. A.; Boast, S.; Goff, S. P.; Lemischka, I. R. *Immunity* **1995**, *3*, 147.
5. Stacchini, A.; Fubini, L.; Severino, A.; Sanavio, F.; Aglietta, M.; Piacibello, W. *Leukemia* **1996**, *10*, 1584.
6. Quentmeier, H.; Reinhardt, J.; Zaborski, M.; Drexler, H. G. *Leukemia* **2003**, *17*, 120.
7. Yamamoto, Y.; Kiyoi, H.; Nakano, Y.; Suzuki, R.; Kodera, Y.; Miyawaki, S.; Asou, N.; Kuriyama, K.; Yagasaki, F.; Shimazaki, C.; Akiyama, H.; Saito, K.; Nishimura, M.; Motoji, T.; Shinagawa, K.; Takeshita, A.; Saito, H.; Ueda, R.; Ohno, R.; Naoe, T. *Blood* **2001**, *97*, 2434.
8. Nakao, M.; Yokota, S.; Iwai, T.; Kaneko, H.; Horiike, S.; Kashima, K.; Sonoda, Y.; Fujimoto, T.; Misawa, S. *Leukemia* **1996**, *10*, 1911.
9. Mizuki, M.; Fenski, R.; Halfter, H.; Matsumura, I.; Schmidt, R.; Muller, C.; Gruning, R.; Kratz-Abers, K.; Serve, S.; Steur, C.; Buchner, T.; Kienast, J.; Kanakura, Y.; Berdel, W. E.; Serve, H. *Blood* **2000**, *96*, 3907.
10. Gale, R. E.; Green, C.; Allen, C.; Mead, A. J.; Burnett, A. K.; Hills, R. K.; Linch, D. C. *Blood* **2008**, *111*, 2776.
11. Kiyoi, H.; Yanada, M.; Ozekia, K. *Int. J. Haematol.* **2005**, *82*, 85.
12. Heinrich, M. C. *Mini-Rev. Med. Chem.* **2004**, *4*, 255.
13. O'Farrell, A.-M.; Abrams, T. J.; Yuen, H. A.; Ngai, T. J.; Louie, S. G.; Yee, K. W.; Wong, L. M.; Hong, W.; Lee, L. B.; Town, A. *Blood* **2003**, *101*, 3597.
14. Zhang, W.; Konopleva, M.; Shi, Y.-X.; McQueen, T.; Harris, D.; Ling, X.; Estrov, Z.; Quintás-Cardama, A.; Small, D.; Cortes, J. *J. Natl. Cancer I* **2008**, *100*, 184.
15. DeAngelo, D. J.; Stone, R. M.; Heaney, M. L.; Nimer, S. D.; Paquette, R. L.; Klisovic, R. B.; Caligiuri, M. A.; Cooper, M. R.; Lecerf, J.-M.; Karol, M. D. *Blood* **2006**, *108*, 3674.
16. Smith, B. D.; Levis, M.; Beran, M.; Giles, F.; Kantarjian, H.; Berg, K.; Murphy, K. M.; Dauses, T.; Allebach, J.; Small, D. *Blood* **2004**, *103*, 3669.
17. Stone, R.; De Angelo, J.; Galinsky, I.; Estey, E.; Klimek, V.; Grandin, W.; Lebwohl, D.; Yap, A.; Cohen, P.; Fox, E. *Ann. Haematol.* **2003**, *83*, S89.
18. Shiotsu, Y.; Kiyoi, H.; Ishikawa, Y.; Tanizaki, R.; Shimizu, M.; Umehara, H.; Ishii, K.; Mori, Y.; Ozeki, K.; Minami, Y. *Blood* **2009**, *114*, 1607.
19. Fathi, A. T.; Chabner, B. A. *Oncologist* **2011**, *16*, 1162.
20. Smith, C. C.; Wang, Q.; Chin, C.-S.; Salerno, S.; Damon, L. E.; Levis, M. J.; Perl, A. E.; Travers, K. J.; Wang, S.; Hunt, J. P. *Nature* **2012**, *485*, 260.
21. Zarrinkar, P. P.; Gunawardane, R. N.; Cramer, M. D.; Gardner, M. F.; Brigham, D.; Belli, B.; Karaman, M. W.; Pratz, K. W.; Pallares, G.; Chao, Q. *Blood* **2009**, *114*, 2984.
22. Kumar, P.; Meenakshi; Kumar, S.; Kumar, A.; Hussain, K.; Kumar, S. *J. Heterocycl. Chem.* **2012**, *49*, 1243.
23. Kitamura, Y.; Sako, S.; Tsutsui, A.; Monguchi, Y.; Maegawa, T.; Kitade, Y.; Sajiki, H. *Adv. Synth. Catal.* **2010**, *352*, 718.
24. Ono, M.; Cheng, Y.; Kimura, H.; Cui, M.; Kagawa, S.; Nishii, R.; Saji, H. *J. Med. Chem.* **2011**, *54*, 2971.
25. Chao, Q.; Sprankle, K. G.; Grotzfeld, R. M.; Lai, A. G.; Carter, T. A.; Velasco, A. M.; Gunawardane, R. N.; Cramer, M. D.; Gardner, M. F.; James, J. *J. Med. Chem.* **2009**, *52*, 7808.